Indian Journal of Engineering & Materials Sciences
Vol. 30, February 2023, pp. 154-164
DOI: 10.56042/ijems.v1i1.65437

Optimisation of Diffusion Welding Parametersin Al-Cu Bimetal for Shaped Charge Application

Santosh Ingole*, MJ Rathod
[1]Department of Metallurgy and Material Science,
College of Engineering Pune, Shivajinagar, Pune 411 005, India

Received: 10 August 2022; Accepted 28 October 2022

Optimum process parameters (temperature, pressure, and time) for diffusion welding of aluminium and copper have been achieved with better shear strength for application in shaped charges using the Taguchi method. The study involved characterising the type thickness of intermetallic compounds formed at the faying surfaces using optical microscopy, scanning electron microscopy and electron probe micro analyser, lap shear strength assessment, microhardness, and X-ray diffraction. It is confirmed that intermetallic compounds of type $Al_4Cu(\sigma)$, Al_2Cu (θ),and AlCu (η_1)with traces of Al_2Cu_3 (δ) and $AlCu_4$ (α_2) were formed at the interface. The optimum shear strength of 42.2 N was achieved with diffusion welding at temperature 510^{o}C, pressure 0.5MPa and time 5400s.By diffusion welding at these conditions, the shape charge cones fabricated and explosively filled such shaped charges paved, an increase of 0.42 times in the penetration of target with diffusion welded copper-aluminium shape charge cones compared with that from conventional monolithic copper sheet.

Keywords: Bimetallic liner, Diffusion welding, Intermetallic compound, Lap shear strength, Shaped charge

1 Introduction

The aluminum and copper joints are used in electrical circuitry/switches[1,2] Solid state diffusion welding produces coalescence at a temperature below the solidus point. Shaped-charge warheads with lining cones made of pure copper sheets are predominantly used owing to their high density and ductility[3]. In order to achieve optimum penetration in the target material, it is necessary to get a high-density jet with mass concentrated at the tip[3]. The conical liner of the shape charge warhead undergoes heavy plastic deformation at a high-speed rate under the sharp rise in pressure associated with implosion[3]. As per the thumb rule in shaped charges, the frontal portion, also called the jet is responsible for penetration with high density and jet tip velocity, whereas the rear part, also called a slug, is responsible for retarding the jet velocity. The maximum mass of cone material goes into the slug. A simulation study has also indicated that by using dissimilar layered copper -aluminum combinations for the shaped charge cones instead of monolithic copper will form a copper-rich jet with heavy mass and aluminum-rich slug due to implosion deformation[3].

Therefore, it was intended to join copper and aluminum sheets by diffusion welding and utilise the dissimilar joined sheet for shaped charge applications.

In the case of similar material joining, diffusion welding produces coalescence at temperatures below solidus temperature when moderate pressure is applied for sufficient time[4,5]. On applied pressure, there is the local plastic deformation of the asperities in contact with the faying surfaces. Solid state diffusion of atoms takes place at these contact points by the mechanisms along the surface and grain boundaries. This process reduces void volume at the interface, improving the bonding. The voids can be eliminated when subjected to prolonged contact, improving the bond strength[6]. Diffusion welding does not involve melting or interface distortion; microstructure and parent metal properties are retained. In the case of diffusion bonding of dissimilar materials, intermetallic compounds may be formed at the interface depending on the chemical potential observed in the binary phase diagram. Thickness and the type of intermetallic compound being brittle or ductile decide the bond strength. A brittle intermetallic compound at the interface makes the joint brittle resulting in poor strength. It has been reported that the diffusion welding temperature should be between 0.5 to 0.7 times the melting point

*Corresponding author:
(E-mail: ingolesn14.meta@coep.ac.in)

or solidus temperature of the lowest melting point material[7].

Since diffusion welding of copper to aluminum sheets is being investigated, the binary phase diagram of copper aluminum is referred to in Fig. 1[8]. It shows a series of different intermetallic compounds which may form at the interface of the copper-aluminum Diffusion welded joint. The diagram also indicates that the diffusion welding temperatures should be 573-773K (300-500°C). This temperature range covers intermetallic compounds like Al_4Cu_9 (γ_2), Al_2Cu_3 (δ), Al_3Cu_4 ($\zeta 2$), AlCu (η_2) and Al_2Cu (θ) [8-13]. Moderate IMC growth may achieve bonding and bond strength. However, excessive IMC growth may lead to a brittle welding interface and bonding failure. Interdiffusion between copper and aluminum is initially taking place, with the formation of α-Al dendrites and intermetallic compounds (IMCs) at the interface[14]. It is revealed that the Al_2Cu starts to concentrate on the copper side due to its composition and tetragonal morphology[15]. Further, by a spinodal decomposition resulting from the concentration gradient, AlCu and Al_4Cu_9 were formed[16].

The present work decided to conduct the diffusion welding of aluminum and copper sheets and study the microstructural changes at the interface. Estimating the Diffusion welded joint strength between aluminum and copper was also decided. Further, the technology outlined is used to bond the flow-formed cones fabricated from aluminum and copper to be utilised for the shaped charge warheads.

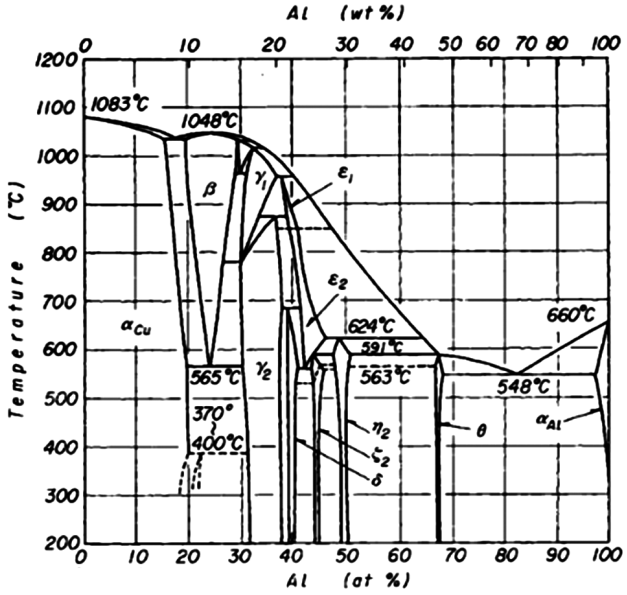

Fig. 1 — Equilibrium phase diagram of Al-Cu System[8].

2 Materials and Methods

Diffusion welding of commercially pure aluminum and electrical grade copper sheets of 2 mm thickness each was performed at 480-540°C temperature with different holding times between 3600 and 1440 second under varying pressures in the range of 0.2 to 0.8 MPa. Intermetallic compounds formed at the interface were studied using optical and scanning electron microscopy and electron probe microanalyzer (EPMA). The impact of the process parameters on the lap shear strength was studied in the interface structure. The optimisation of the joint shear strength was studied concerning process parameters using the Taguchi method. Microhardness traverse was carried out across the interface. After the lap shear test, the surfaces and the intermetallic compounds were identified using X-ray diffraction (XRD).

2.1 Materials and pre-treatment

A copper sheet of 2 mm thickness of oxygen-free electrolytic grade -IS 191 was used to join with the 2 mm thick sheet of aluminum having grade IS737 (designation 19000). The sheets were cut to 15 mm in width and 75 mm in length. The faying surfaces of the sheets were ground with 100 grit emery paper. Just before diffusion welding, the surfaces of the specimen were chemically cleaned to get rid of the oxide layer, oil, or dirt. A solution of 10% Na_2CO_3 and 5% dilute HNO3 in water was used for cleaning aluminum sheets, whereas copper sheets were washed with 28% dilute HNO_3 and 1% HF in water.

2.2 Diffusion Welding

It was decided to perform diffusion welding of the dissimilar sheets with an overlap area of about 15 mm width and 25 mm length. A hot power machine (BEMCO, 100-ton force capacity) was used for diffusion welding, having a die-punch assembly with the provision of isostatic pressing (Fig. 2). The 2kW resistance heating jacket surrounds the die-punch assembly attached with a K-type thermocouple and further connected with temperature indicator and controller.

The experimental layout uses Taguchi's Orthogonal Array (L9) for three variables to optimise the DB parameters (Table 1)[17-18]. This array satisfies the optimum number of experimental conditions with the factors/levels (Table 1). Further, the data was examined using Minitab17 software [19] to obtain the S/N ratio and mean, which provides optimum conditions for Diffusion welding of the Al-Cu.

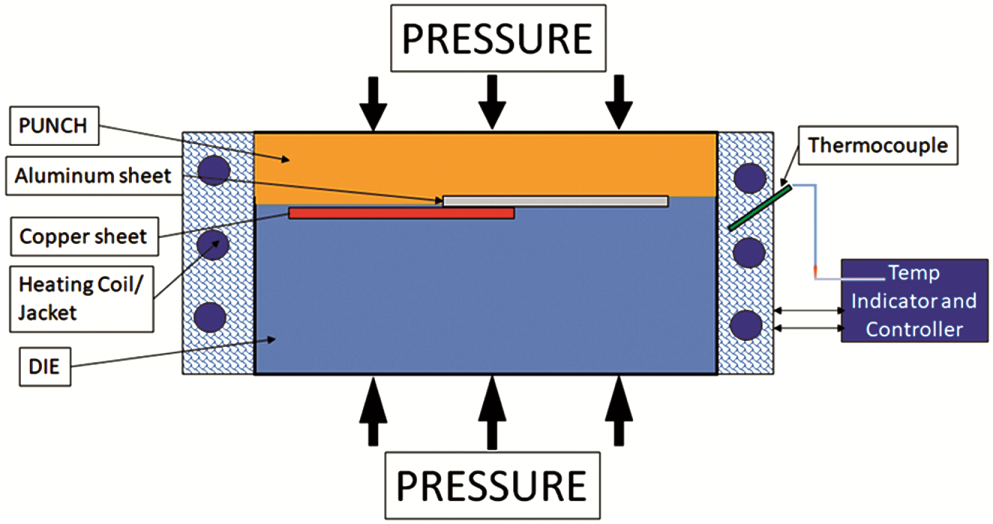

Fig. 2 — Setup for diffusion welding.

Table1 — Variable and its significance index

Parameter	Unit	Parameter Designation	Taguchi's significance Index		
			1	2	3
Pressure	MPa	A	0.8	0.5	0.2
Temperature	°C(K)	B	540 (813)	510 (783)	480 (753)
Time	S	C	14400	9900	5400

Note: A1=0.8MPa, B2=510°C &C3=5400 s

2.3 Analysis of diffusion welded specimens

Bonded bimetal surfaces formed after Diffusion of 20mm are cut carefully from the total strips, and the same was cold mounted. All such surfaces were prepared after polishing and chemical etching (aqueous solution in distilled water of 2.5ml concentrated (90%) nitric acid, 1.5 ml of dilute (50%) hydrochloric acid, and 1.0ml concentrated (65%) hydrofluoric acid). Mounting is analysed under a 50/100X optical microscope for different phases, bonding zone, etc. In order to ascertain the microstructure of bonded surface, the mount was examined using an in-lens detector of a Field Emission Scanning Electron Microscopy (FESEM- Carl-Zeiss Merlin make)-40kV with an accelerating voltage of 5kV. The composition of IMC was evaluated using an Energy Dispersive X-ray Spectroscopy (EDS-Oxford make) at an accelerating voltage of 20kV.

CAMECA equipment has been utilised for EPMA of Diffusion welded sample.[20] The material under investigation is bombarded with a beam of energy sufficient electrons to knock out electrons from the inner orbital of the atoms comprising the material".

Microhardness of the cold mounted samples were measured with Zeiss-Micro Vickers hardness tester

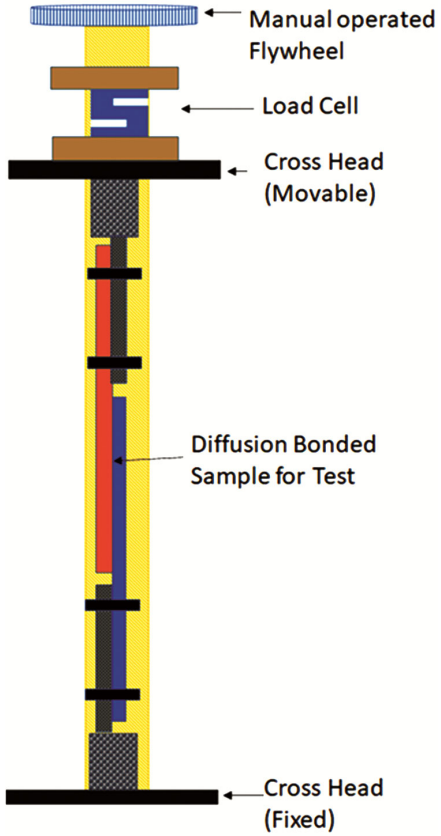

Fig. 3 — Setup for measurement of lap shear strength.

@25g load as per ASTM E384[21]. Hardness-traverse across the interfaces and their surrounding regions has been reported in the form of a microhardness profile.

Diffusion welded sample subjected to Lap shear strength measurement (Fig. 3) using principles of ASTM D1002[22] using a manually operated spring

Table 2 — Sample Distribution for Analysis

Exp. No.	Parameter & Significance			Detection/Analysis Method					
				OM	EDS	EPMA	LS	MH	X-ray diffraction
X1	a1	b1	c1	*S*	*S*	*S*	*S*	*N*	*N*
X2	a1	b2	c2	*S*	*N*	*S*	*S*	*N*	*N*
X3	a1	b3	c3	*S*	*S*	*S*	*S*	*S*	*S*
X4	a2	b1	c2	*S*	*S*	*S*	*S*	*N*	*S*
X5	a2	b2	c3	*S*	*S*	*S*	*S*	*N*	*S*
X6	a2	b3	c1	*S*	*S*	*S*	*S*	*N*	*S*
X7	a3	b1	c3	*S*	*S*	*S*	*S*	*N*	*S*
X8	a3	b2	c1	*S*	*S*	*S*	*S*	*N*	*S*
X9	a3	b3	c2	*S*	*N*	*S*	*S*	*N*	*S*

Note1. :S -Subjected & N- Not subjected for analysis
Note2.: This table is to be read with Table 2 to get the Experimental condition
*e.g., for Experiment X4= =(a2, b1, c3)= = Pressure (0.5 MPa), Temperature(540^{o}C), time(540**0s)***

Table 3 — Criteria for Intermetallic solid solution for Al-Cu system

Criteria	Applicability for Al & copper	Remarks
Atomic Size factor (ASF) : $\left\|\frac{r_1 - r_2}{r_1}\right\| \leq 0.15$	Al :118pm &Cu : 145pm ASF=0.18 > 0.15	Solubility possible but he lattice strain hinders the solubility
Crystal Structure : Should be same	Al& Cu both FCC	Meets the requirement
Electronegativity potential/ difference (ENP): $\left\|\frac{x_1 - x_2}{x_1}\right\| \leq 0.3$	Al:1.61 & Cu:1.90 ENP=0.15<0.3	Due to less ENP formation of intermetallic compound is possible
Similar Valency	Al: 3 & Cu:2/1 Valency difference=1 or 2	Maximum solubility possible with similar valency

test apparatus with load cell and digital load/deflection indicator.

Fractured surfaces after lap shear strength assessment are analysed with X-ray diffraction. Copper and aluminum samples separated after lap shear strength were subjected to X-ray diffraction individually. D8-Advance (Make: Bruker AXS GmbH) has a 40kVA source; X-ray Diffractometer. X-ray diffraction was carried out with: diffraction angle: 20-80^{o}; Radiation: Cu-Kα; Step Size: 10s; and Scan speed: 0.01°. Peak indexing, identification of the phases, and lattice parameters of intense peaks can be assessed using the Joint Commission on Powder Diffraction (JCPD) database [23]. Further, the results were analysed using X'Pert Highscore & Origin8.5 application software.

2.4 Penetration Trials using bimetallic lined shaped charge

Explosive filled shaped charges with monolithic (only copper) and bimetallic lined shaped charges have been subjected to penetration trials [3]. Here, flow-formed conical liners made from aluminum and copper sheet have been Diffusion welded with the technology outlined in the ibid research work[24]. These explosive-filled charges had been subjected to penetration trial with MS block as the target to ascertain the penetration performance. High-speed videography provided velocity profiles.

3 Results and Discussion

3.1 Thermodynamics of Intermetallic complex formation in diffusion bonding of Al-Cu

The possibility of formation of solid solution in Al-Cu system has been confirmed as outlined in Hume-Rothery rules [25-26] and same is reproduced in Table 3.

Form the Bene Rule for metal-metal nucleation, it revealed that the nucleated first phase of solid-state diffusion is the one which is in immediate vicinity of eutectic at low temperature in the phase diagram[27]. In such interactions, after first phase formation, the next phase is with most negative effective heat of formation (EHF) pertaining to the interface between the compound phase as well as remaining element phase which are rich in the unreacted element[28]. Present study conducted between the temperature range of 480-540^{O}C (753-813K).

EHF model developed by Pretorius *et al* [28] is used to predict formation of first phase in Al-Cu binary system. Based in this model the EHF, $\Delta H^{l}$is defined as [29]:

$$\Delta H^l = \Delta H^O x \frac{C_e}{C_l} \quad \ldots (1)$$

Where, ΔH^O the standard heat of formation[29]; $C_e$is limiting element effective concentration (which will be used up first during formation of one phase) at the interface, taken as the composition of limiting element at lowest eutectic temperature. C_l is limiting element concentration in the compound. Therefore, using thermodynamic data EHF has been calculated and listed in Table 4. Also, as per the sub-regular solution model (SRSM)[30-32] Molar Gibbs free energy of FCC phase (both Cu & Al rich phases) can be obtained as below:

$$G^s = G^s_{Al}(1-x) + G^s_{Cu}x + RT[x\,lnx + (1-x)\ln(1-x)] + x(1-x)[L^s_0 + L^s_1(1-2x) + L^s_2(4x^2-4x+1)] \quad \ldots (2)$$

Where, s stands for solid phase; x is the mole fraction of Cu; G^s is the Gibbs free energy of pure metal; L^s_0, L^s_1, L^s_2 are interaction coefficients which are related to the temperature. Gibbs free energy calculation formulas of Cu & Al solid phase of FCC are respectively as follows:

$$G^S_{Al} = -7976.15 + 137.093038T - 24.3671976T\ln(T) - 1.884662E^{-3}T^2 - 0.877664E^{-6}T^3 + 74092T^{-1} \quad \ldots (3)$$

$$G^S_{Cu} = -7770.458 + 130.485235T - 24.112392T\ln(T) - 2.65684E^{-3}T^2 + 0.129223E^{-6}T^3 + 52478T^{-1} \quad \ldots (4)$$

And interaction coefficients in solid phase:

$$L^s_0 = 53520 + 2T \;;\; L^s_1 = 38590 - 2T \;;\; L^s_2 = 1170 + 2T \quad \ldots (5)$$

Molar Gibbs free energy calculated from equation (2) for various IMC under consideration are tabulated in Table 5. From this EHF model, the values of ΔH^l were calculated for all the five intermetallic phases. It can be seen that AlCu(η_1) has the highest negative EHF and has tendency for preferential formation in the diffusion zone. This result confirms the first nucleation of AlCu in view of thermodynamics combined with kinetic theory, as also subsequent possibility of formation of IMCs in the order σ, θ, η_1, ζ_1, χ, δ, γ_2 , α_1, α_2 and αCu. Further on the basis of Gibs free energy, for all experimental temperatures, sequence of formation of IMC is σ, θ, η_1, ζ_1, δ, χ, γ_2 , α_1, α_2 and αCu.

3.2 Qualitative /Quantitative analysis of IMC

(i) Analysis summary is described in Table 5.

(ii) Optical microscopic images at 50X/100X (Fig. 4) magnification; depicts formation of intermetallic complex (IMC). Under this observation, it is derived that the Thickness of IMC formation has remarkable variation. The microhardness of the samples is shown in Fig. 5, and variation in the microhardness curve also confirms IMC formation at the interface. SEM/EDS micrograph/image of Diffusion welded sample is shown in Fig. 6. IMC composition and thickness are measured.BSE image and EPMA scan results are reproduced in Fig. 7. Whereas, Fig. 8 are the XRD peaks of the Copper and Aluminium side of the same samples.

(iii) Thickness of interlayer varies from 12 μm to 197μm.

(iv) X_1 (Pressure 0.8MPa, Temp. 540^{O}C, and holding time 14400s) shows the formation of δ & α_2 phases and interface thickness of 8.5-16.7μm with resultant negligible Lap shear strength (9.8N).

(v) X_2 (Pressure 0.8MPa, Temp. 510°C and holding time 9900s) shows the formation of γ_2, δ, η_1, α_1, σ phases and interface thickness of 14-23μm with resultant negligible Lap shear strength (9.8N).

Table 4 — EHF and Gibbs free energy for intermetallic complexes in Al-Cu System

IMC/Phase		Mole fraction of copper	Standard Heat of Formation ΔH^O(kJ/mole) [31]	EHF ΔH^l (kJ/mole) (Eq. 1)	Gibbs free energy for mixture (kJ/mole) (Eq.2) at Temperature (K)		
					753 K	783 K	813 K
γ_2	Cu_9Al_4	0.692	-21.69	-5.61	-297.659	-328.756	-361.993
δ	Cu_3Al_2	0.6	-20.67	-5.84	-396.002	-439.128	-485.359
ζ_1	Cu_4Al_3	0.552	-20.40	-6.29	-447.030	-496.427	-549.432
η_1	$CuAl$	0.498	-19.92	-6.68	-504.094	-560.543	-621.167
Θ	$CuAl2$	0.33	-13.05	-6.76	-678.463	-756.834	-841.141
α_2	Cu_4Al	0.8	-13.92	-3.11	-181.854	-198.815	-216.783
α_1	Cu_3Al	0.75	-18.43	-4.4	-235.474	-258.981	-284.021
X	$Cu_{6.108}Al_{3.892}$	0.61	-20.67	-6.07	-385.343	-427.161	-471980
αCu	$Copper$	0.765	-12.73	-2.98	-219.386	-240.929	-263.848
Σ	$CuAl_4$	0.20	-8.5	-7.61	-809.603	-904.915	-1007.526
Favoured Formation sequence of intermetallic compounds					σ, θ, η1, ζ1, δ, χ, γ2, α1, α2 and αCu		

Table 5 — Analysis Summary of diffusion welded Samples

Sample No.	Analysis method	Detection of intermetallic complexes									The thickness of the IMC phase (μm)	Lap Shear Strength (N)
		Al_2Cu (θ)	Cu_9Al_4(γ_2)	Al_2Cu_3(δ)	AlCu (η_1)	$Al_{3.892}Cu_{6.10808}$ (χ)	$AlCu_3$(α_1)	Cu_3Al_2(δ)	$AlCu_4$(α_2)	Al_4Cu(σ)		
X1	EDS	*Z*	*Z*	*D*	*Z*	*Z*	*Z*	*Z*	*D*	*Z*	14.3-16.7	9.8
	OM	-	-	-	-	-	-	-	-	-	8.5-16.3	
X2	EPMA	*Z*	*D*	*Z*	*D*	*Z*	*D*	*D*	*Z*	*D*	15-23	9.8
	OM	-	-	-	-	-	-	-	-	-	14-22	
X3	XRD	*D*	*D*	*Z*	*Z*	*Z*	*Z*	*Z*	*Z*	*Z*	-	42.17
		D	*D*	*Z*	*Z*	*Z*	*Z*	*Z*	*Z*	*Z*	-	
	EDS	*D*	*Z*	*D*	*D*	*Z*	*Z*	*Z*	*D*	*Z*	12.1-15.3	
	OM	-	-	-	-	-	-	-	-	-	65-79	
X4	XRD	*D*	*Z*	*Z*	*Z*	*D*	*D*	*D*	*D*	*Z*	-	9.8
		Z	*D*	*Z*	*D*	*D*	*Z*	*Z*	*D*	*Z*	-	
	EDS	*D*	*Z*	*Z*	*D*	*Z*	*D*	*Z*	*Z*	*Z*	95.6	
	EPMA	*Z*	*D*	*Z*	*D*	*Z*	*D*	*D*	*Z*	*D*	15-23	
	OM	-	-	-	-	-	-	-	-	-	86-116	
X5	XRD	*D*	*Z*	*Z*	*Z*	*Z*	*Z*	*Z*	*Z*	*Z*	-	70
		Z	*D*	*Z*	*Z*	*D*	*Z*	*D*	*D*	*Z*	-	
	EDS	*Z*	*Z*	*Z*	*D*	*Z*	*Z*	*Z*	*Z*	*Z*	16.6-22	
	OM	-	-	-	-	-	-	-	-	-	23-28	
X6	XRD	*D*	*D*	*Z*	*Z*	*Z*	*Z*	*Z*	*Z*	*Z*	-	9.8
		D	*D*	*Z*	*Z*	*D*	*D*	*Z*	*D*	*Z*	-	
	OM	-	-	-	-	-	-	-	-	-	138-165	
X7	XRD	*D*	*Z*	*Z*	*D*	*D*	*D*	*Z*	*D*	*Z*	-	9.8
		D	*D*	*Z*	*Z*	*D*	*Z*	*Z*	*Z*	*Z*	-	
	EDS	*Z*	*Z*	*Z*	*Z*	*Z*	*Z*	*Z*	*Z*	*D*	183-197	
	OM	-	-	-	-	-	-	-	-	-	63-82	
X8	XRD	*D*	*D*	*Z*	*Z*	*Z*	*D*	*Z*	*D*	*Z*	-	9.8
		D	*D*	*Z*	*Z*	*D*	*Z*	*Z*	*D*	*Z*	-	
	EDS	*Z*	*D*	*D*	*D*	*Z*	*Z*	*Z*	*D*	*D*	11.5-18.8	
	OM	-	-	-	-	-	-	-	-	-	15-23	
X9	XRD	*D*	*D*	*Z*	*Z*	*Z*	*D*	*Z*	*Z*	*Z*	-	21.82
		Z	*D*	*Z*	*Z*	*Z*	*Z*	*Z*	*D*	*Z*	-	
	OM	-	-	-	-	-	-	-	-	-	17-22	

Note1: D- Detection of IMC; Z- Non-detection of IMC

(vi) X_4 (Pressure 0.5MPa, Temp. 540°C and holding time 14400s) shows the formation of θ, γ_2, η_1, χ, α_1, α_2, σ phases and interface thickness of 15-116μm with resultant negligible Lap shear strength (9.8N).

(vii) X5 (Pressure 0.5 MPa, Temp. 510°C and holding time 9900s) shows the formation of θ, γ2, δ, η1, χ, α2 phases and interface thickness of 16.6-28μm with resultant Lap shear strength of 70N.

(viii) X_6 (Pressure 0.5 MPa, Temp. 480^{O}C and holding time 5400s) shows the formation of θ, γ_2, χ, α_1, α_2 phases and interface thickness of 138-165μm with resultant negligible Lap shear strength (9.8N).

(ix) X_3 (Pressure 0.8MPa, Temp. 480^{O}C and holding time 5400s) shows the formation of θ, γ_2, δ, η_1, α_2 phases and interface thickness of 12.1-79μm with resultant Lap shear strength of 42.17N.

(x) X_7 (Pressure 0.2 MPa, Temp. 540^{O}C and holding time 14400s) shows the formation of θ, γ_2, η_1, χ, α_1, α_2, σ phases and interface thickness of 63-197μm with resultant negligible Lap shear strength (9.8N).

(xi) X8 (Pressure 0.2 MPa, Temp. 510^{O}C and holding time 9900s) shows the formation of θ, γ_2, δ,

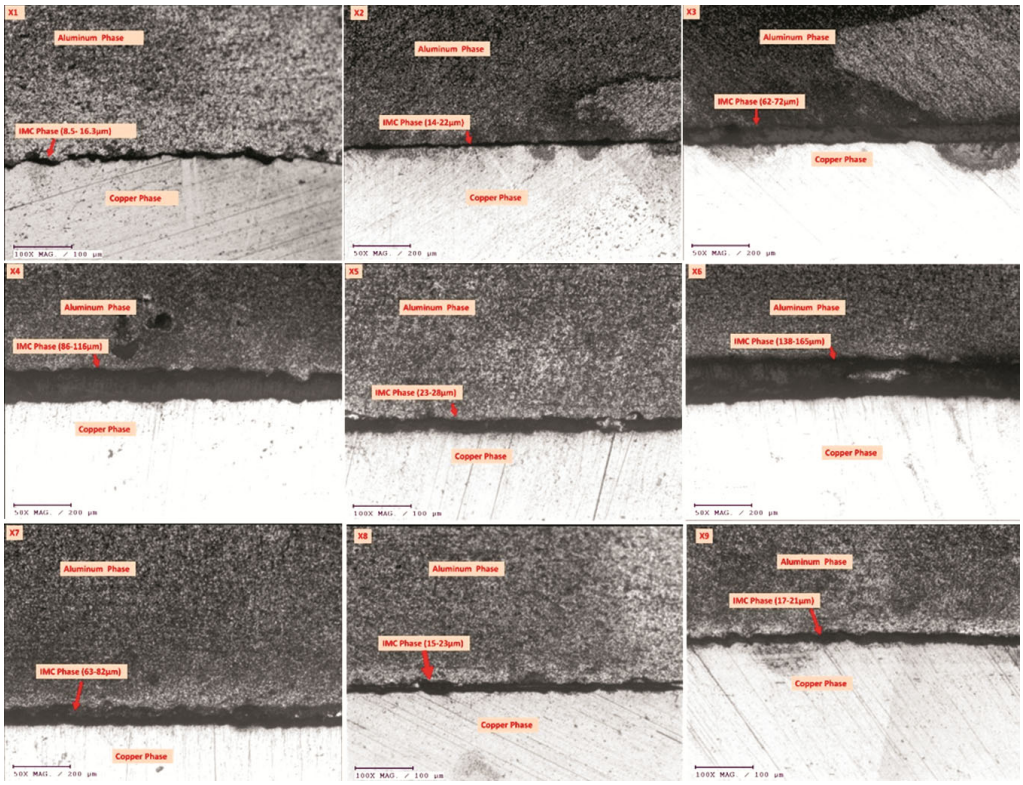

Fig. 4 — Optical Microscopic images of DB Samples DB Sample (at Different processed conditions): (a) X1 (0.8 MPa, 540° c, 14400s); (b) X2 (0.8 MP, 510° C, 9900s), (c) X3 (0.8Mpa,480°C, 5400s), (d) X4 (0.5Mpa, 540° C, 14400s, (e) X5 (0.5MPa, 510° C, 9900s, (f) X6 (0.5 MPa, 480° C 5400s), (g) X7 (0.2 MPa, 54° C, 1400s, and) (h) X8 (0.2MPa, 510° C, 9900s (i) X9 (0.2MPa, 480° C, 5400s).

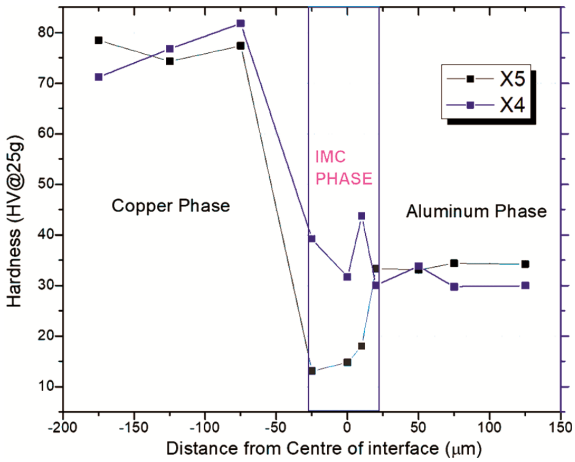

Fig. 5 — Microhardness profile of diffusion welded Samples.

η_1, χ, α_1, α_2, σ phases and interface thickness of 11.5-23µm with resultant negligible Lap shear strength (9.8N).

(xii) X_9 (Pressure 0.2 MPa, Temp. 480°C and holding time 5400s) shows the formation of θ, γ_2, α_1, α_2 phases and interface thickness of 17-22µm with resultant Lap shear strength of 21.82N.

(xiii) Lap shear strength of DB Samples is given in Table 5. It is found that X3, X5, and X7 exhibit substantial Lap shear strength (42.17N, 70N, and 21.82N, respectively).

3.3 Optimisation of DB parameters

In order to obtain Optimum Diffusion bonding parameters, the experiments were designed using the L9 Orthogonal Array of Taguchi (with observed values as per Table 1,2,5 for each parameter and further computed using Minitab17 for Signal to Noise (S/N) ratio & mean. Table 6 & Fig. 9 shows the S/N ratio & mean as Taguchi analysis, considering that- more significant is better optimised.

Bonding temperature improves the contact ratio and shear strength[30,31]. At lower temperature, tendency of metal flow is low but high yield strength of base metals resulting into transient, yet incomplete coalescence of diffusion product. With increased temperature, brittle intermetallic compounds increase its span of width thereby over-balances the positive effect due to betterment in amalgamated faying surfaces. Shear strength/bond strength of the joints has tendency to rise with applied pressure for bonding. Therefore, when the bonding pressure is applied, the points of contact between the two surfaces expands almost instantaneously. At lower bonding pressure, contact

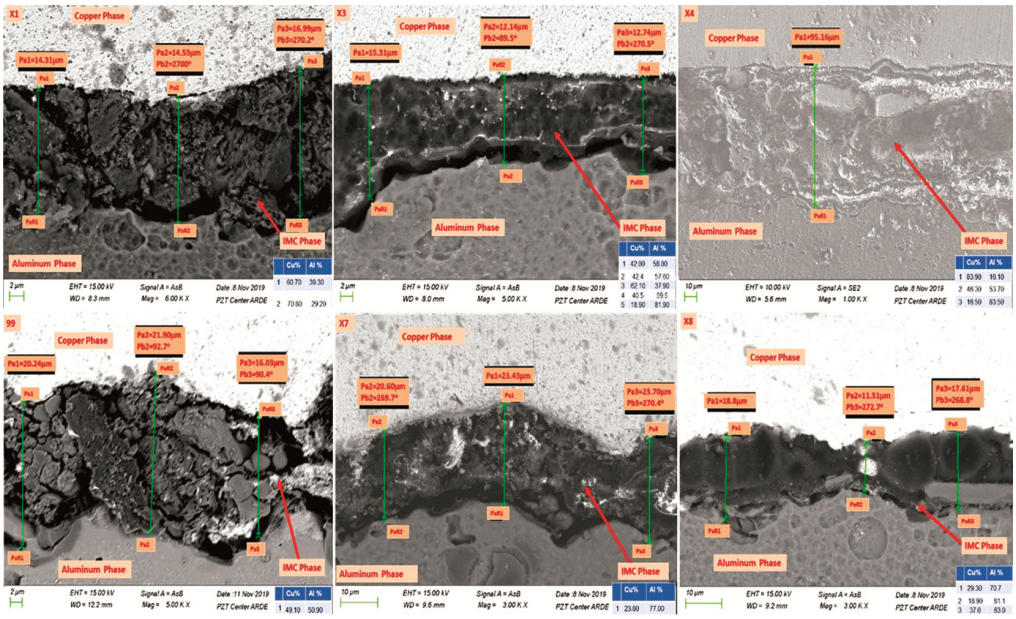

Fig. 6 — SEM Images of welded samples (at Different processed conditions) (a) X1 (0.8 MPa, 540° C, 1400s) (b) X3 (0.8 MPa, 480° C, 5400s) (c) X4 (0.5MPa, 540° C, 1400s) (d) X5 (0.5MPa, 510s, 9900s (e) X7 0.2 MPa, 540s, 14400s), (f) X8 (0.2 MPa, 510 ° C, 9900s).

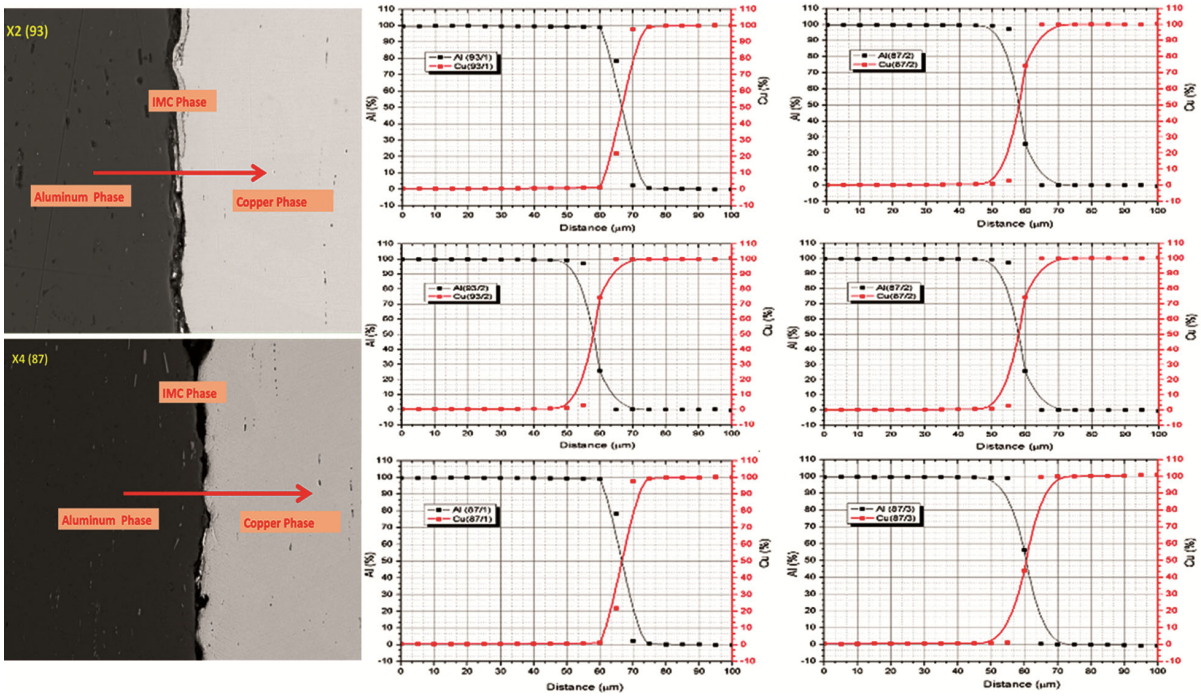

Fig. 7 — BSE image and EPMA Scan of diffusion welded Sample.

is only at the protrusions on the bonded surface, so the contact rates and the strength of the bonded joint are lower, while increase in pressure can develop plastic deformation at contact surfaces. Increase in pressure responsible for recrystallisation, increased rate of interface contacts and movement of atoms as well as voids termed as Kirkendall effect [32]. Larger Voids can be reduced with smaller voids subject to stress within the contact zone by conventional creep or plasticity. Holding time influences the creep of the protrusions and the quantity of atomic diffusion [33]. Shear strength of the joint increases with increasing holding time. If holding time is insufficient, diffusion as also formation of IMC would be lower,

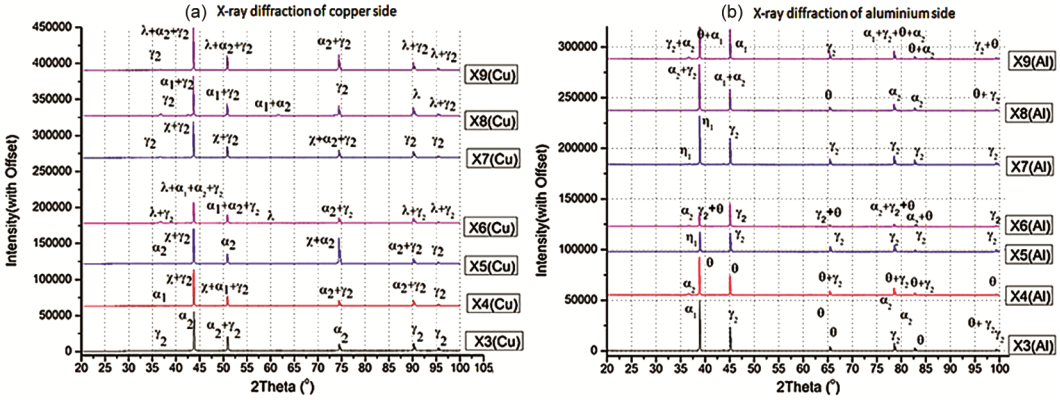

Fig. 8 — XRD Analysis of Cu and Al Sample.

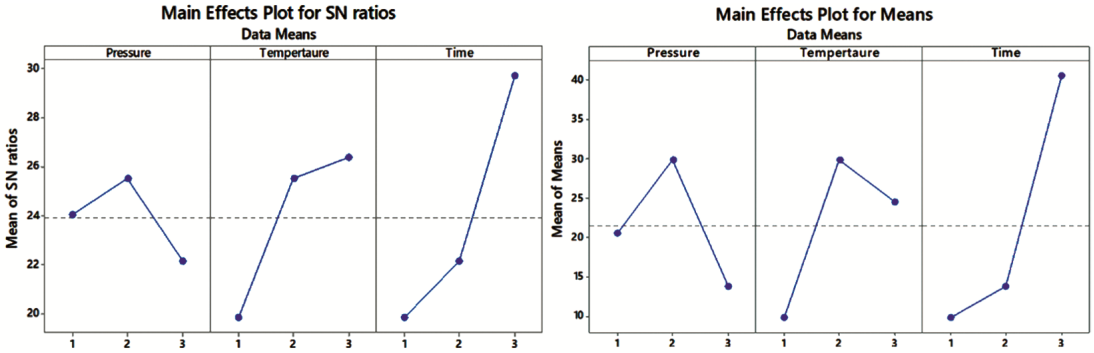

Fig. 9 — Main effects plot for S/N Ratio and means.

Table 6 — Response Table for Signal to Noise Ratios & Means

Level	S/N Ratio			Means		
	Pressure (MPa)	Temperature (°C)	Time (s)	Pressure (MPa)	Temperature (°C)	Time (s)
1	2.45	19.82	1189.2	2.059	9.8	1189.2
2	2.552	25.52	1328.4	2.9867	29.867	828.42
3	2.214	26.37	1784.4	1.3807	24.597	2439.42
Delta	3.37	6.54	9.92	16.06	20.067	30.857
Rank	3	2	1	3	2	1

Table 7 — Performance after Penetration Trials

Charge Configuration	Performance		Remarks
	Penetration Depth (mm)	Jet Tip Velocity (m/s)	
Monolithic	190mm	6700m/s	42% increase in Penetration and 19% increase in Jet tip Velocity
Bimetallic	270mm	8000m/s	

thus lowering the bond strength. Contrary larger holding time is useful optimally in terms of strength and beyond which not useful as leads to formation of brittle compounds (IMC).

Thus, the Diffusion welding parameters which results in providing maximum Bond/lap shear strength are :

Pressure : 0.5 MPa
Temperature : 510°C
Time : 5400s

3.4 Performance of bimetallic lined shaped charges

The explosive-filled shaped charges, when subjected to penetration on mild steel target under identical conditions to ascertain the penetration performance, jet tip velocity revealed that bimetallic lined shaped-charge provide 0.42 times higher penetration compared to monolithic lined shaped charge with 0.19 times higher jet tip velocity (Table 7). The Collapse of the bimetallic liner is depicted in Fig. 10. The collapse analysis reveals that

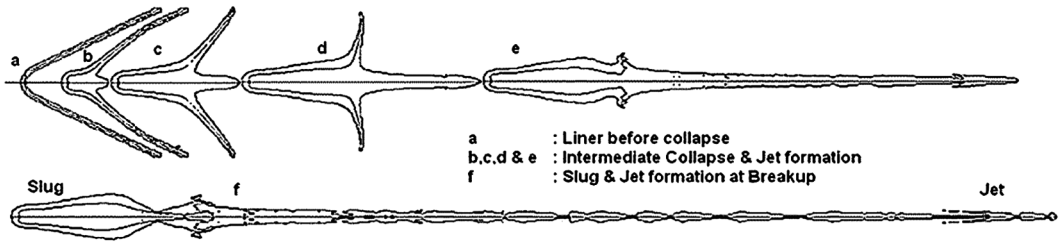

Fig. 10 — Collapse of Bimetallic liner during penetration studies [24].

the aluminum in contact with the explosive remains mainly in the slug. In contrast, the heavy copper goes into the slug, thereby responsible for high mass, velocity, and momentum for penetration into the target.

4 Conclusion

From the Present study on Al-Cu diffusion welding, it is concluded that:

(i) Qualitative/Quantitative Characterisation (Microstructure, Microhardness, SEM/EDS, EPMA, XRD) of Diffusion boded samples confirmed the formation of intermetallic complexes. Owing to the property of intermetallic, it contributes cumulatively to the bond strength of materials.

(ii) Formation of Intermetallic complexes or phases (σ, θ, η_1, ζ_1, δ, χ, γ_2, α_1, α_2) with varied interlayer thickness has been studied and confirmed.

(iii) Study of Diffusion welding for Al-Cu sheets under different conditions, which are selected based on the phase diagram, has been carried out. The parameters are responsible for achieving higher Lap shear strength which indirectly states the bonding strength of Diffusion bonded material has been optimised.

(iv) Larger bond strength achieved at optimum conditions of Pressure: 0.5MPa, Temperature 510^{O}C, and holding time of 5400s.

(v) The Diffusion bonded bimetallic-shaped charge liners provided 42% higher penetration and 19% higher jet tip velocity.

Acknowledgment

We sincerely acknowledge Director COEP, Director ARDE Pune, Director HEMRL Pune, Director DMRL Hyderabad, and Director General DGAQA New Delhi for providing needful support in the present work.

References

1 M Braunovic & N Alexandrov, *IEEE Trans. On Components, Packaging, And Manufacturing Technology*, 17(1) (1994) 78.

2 G. Mahendiran, V Balasubramanian & T Sethilvelan, *J Elixir Mech Engg*, 38 (2011) 4283.

3 Santosh N Ingole, MJ Rathod, KM Rajan, RK Sinha, SK Nayak, Nair Prakash NP, VK Dixit & SG Kulkarni, *Proc 6th International Symposium on Explosion Shock wave and High-strain-rate Phenomena, Puducherry-India, Materials Research Forum LLC, Materials Research Proceedings,* 13(2019) 141.

4 I Galvão, JC Oliveira, A Loureiro & DM Rodrigues, *J Intermetallics*, 22(2012) 122.

5 MJ Rathod & M Kutsuna, *Welding Journal*, 83(1) (2004) 16S.

6 ASM Handbook Vol 6 (1993), 519.

7 FA Calvo, A Urena, JM Gomez de Salazar & F Molleda, *J Material Science*, 23(1988) 2273.

8 Kemal Aydın, Yakup Kaya & Nizamettin Kahraman, *J Materials and Design*, 37(2012) 356.

9 Yasuhiro Funamizu & Katsuya Watanabe, *J Trans Japan Inst of Metals*, 12 (1971) 147.

10 J. L. Murray, *J. International Metals Reviews*, 30 (1985) 211.

11 Norbert Ponweiser, Christian L Lengauer & Klaus W. Richter, *J. Intermetallics*, 19 (2011) 1737.

12 Hyoung-Joon Kim, Joo Yeon Lee, Kyung-Wook Paik, Kwang-Won Koh, Jinhee Won, Sihyub Choe, Jin Lee, Jung-Tak Moon, & Yong-Jin Park, *J IEEE Transactions on Components and Packaging Technologies*, 26(2) (2003) 367.

13 Yajie Guo, Guiwu Liu, HaiyunJin, ZhongqiShi & GuanjunQiao, *J Mater Sci*, 46 (2011) 2467.

14 T Wang, F Cao, P Zhou, H Kang, Z Chen, Y Fu, T Xiao, W Huang & Q Yuan, *J Alloy Compd*, 616(2014) 550.

15 S Tavassoli, M Abbasi & R Tahavvori, *J Mater Des*, 108(2016) 343.

16 D Moreno, J Garrett & J Embury, *J Intermetallics*, 7(1999) 1001.

17 Raghu N Kacker, Eric S Lagergren & James J Filliben, *J Res Natl Inst Stand Technol*, 96(5) (1991) 577.

18 Krishankant, Jatin Taneja, Mohit Bector & Rajesh Kumar, *Int. J Eng and Adv Tech.*, 2(1) (2012) 263.

19 M Honarpisheh, M. Asemabadi & M. Sedighi, *J Materials and Design*, 37 (2012) 122.

20 Rinaldi, Romano & Llovet, Xavier, *Microscopy and Microanalysis*, 21 (2015) 1053. 10.1017/S1431927615 000409.

21 ASTM E384, Standard Test Method for Microindentation Hardness of Materials, (*American Society for Testing and Materials*, *West Conshohocken)* (2011) 1.

22 ASTM D1002, Standard Test Method for Apparent Shear Strength of Single-Lap-Joint Adhesively Bonded Metal Specimens by Tension Loading (Metal-to-Metal), (American Society for Testing and Materials, West Conshohocken*)* (2019) 1.

23 VS Kathavate, B Praveen Kumar, I Singh & K EswarPrasada, *J Ceramics International*, 46 (2020) 12876.

24 Santosh Namdeo Ingole & M J Rathod, *An Improved Shaped Charge Liner*, Indian Patent (Application No.) 202221012974, 10 March 2022.

25 K Janghorban, JS Kirkaldy & GC Weatherly, *J Phys Condens. Matter*, 13 (2001) 8661.

26 HJ Axon, D Phil & W Hume-Rothery, FRS, *Proc of the Royal Society of London Series A, Mathematical Physical Sciences*, 193A (1948) 1.

27 RW Bene, *J App Physics Letters*, 41 (1982) 529.

28 R Pretorius, *J Materials letters,* 9 (12) (1990) 494.

29 John Hair & DB Downie, *J Faraday Symp Chem Soc*, 8(1973) 56.

30 Zuruzi AS & Li H, Dong G, *J Materials Science Engineering A*, A270 (1999), 244.

31 P He & D Liu, *J Materials Science and Engineering A*, 437 (2006) 430.

32 Hidetoshi Somekawa, Hiroyuki Hosokawa, Hiroyuki Watanabe & Kenji Higashi, *J Materials Science and Engineering-A*, A339 (2003) 328.

33 Wang Juan, Li Yajiang, Liu Peng & Geng Haoran, *J Materials Processing Technology*, 205 (2008)146.